Algerian Journal of Chemical Engineering 01 (2020) 31–38

Algerian Journal of Chemical Engineering

Journal homepage: http://www.ajce.periodikos.com.br/

Original Article

Numerical predictions using LBM application: laminar mixed convection of non-Newtonian nanofluids in ventilated square cavities

Abdelkader BOUTRA[a,b]*, Nabila LABSI[b] and Youb Khaled BENKAHLA[b]

[a] *Ecole Supérieure des Sciences Appliquées d'Alger, Algerie*

[b]*Laboratory of Transport Phenomena, USTHB, Algiers, Algeria*

ARTICLE INFO

Article history:
Received 30 August 2020
Revised 23 September 2020
Accepted 18 November 2020

Keywords:
Heat transfer;
Viscoplastic;
Lattice Boltzmann;
Bingham fluid;
Mixed convection.

ABSTRACT

In this paper, we investigate numerically the flow field and heat transfer of a viscoplastic nanofluid flowing within ventilated devices. The incompressible nanofluid with constant and uniform physical and rheological properties is composed of silver nanoparticles suspended in a non-Newtonian base fluid that obeys the Bingham rheological model. This numerical study is based on the multiple-relaxation-time Lattice Boltzmann method (MRT-LBM). The two-dimensional nine-velocity (D_2Q_9) model is adopted to solve the flow field, while the two-dimensional five-velocity (D_2Q_5) model is developed to solve the temperature field. The impact of various pertinent parameters, such as Richardson ($0.01 \leq Ri \leq 100$), Bingham ($0 \leq Bn \leq 20$), and Prandtl numbers ($1 \leq Pr \leq 30$), is widely inspected, side by side with the nanoparticles volume fraction ($0 \leq \varphi \leq 10\%$). The obtained results show the important effect of these parameters, which cannot be neglected, on both flow and heat transfer structures, in this type of cavities.

1. Introduction

Mixed convection in a cavity is relevant to many industrial and environmental applications such as in heat exchangers, nuclear and chemical reactors and cooling of electronic equipments. However, in engineering applications, the geometries that arise are more complicated than simple cavity configurations filled with a convective fluid [1-3].

For cavities, the range of problems that can be analysed is mainly related to the geometric configuration of the cavity and the type of convective flow: natural, forced or mixed. Generally, the geometric cavity configuration encompasses aspects such as: closed or opened cavity, number of openings and its aspect ratio.

In the recent decades, some researchers have developed works focusing on mixed convection in cavities with openings mass flow, commonly called ventilated cavities, crossed by fluids [4-6] and recently, by nanofluids [7-9].

Non-Newtonian nanofluids flow has been investigated for a wide set of thermal conditions. Kamali and Binesh [10] performed a numerical investigation in order to understand the non-Newtonian Carbon Nanotube (CNT) nanofluid behaviour, in the case of the power law model. Moawed et *al.* [11] studied the forced convection of blood-gold (Au) non-Newtonian nanofluid within a tube. Similar studies were conducted by Hojjat et *al.* [12] and Moraveji et *al.* [13].

The importance of recent developments of the flow simulation using the MRT-LBM, motivates the present study [14, 16]. In this paper, the Lattice Boltzmann method, with multiple times of relaxation (MRT-LBM) is developed to simulate convection heat transfer in a ventilated square cavity crossed by a viscoplastic

* *Corresponding author.* Tel.: 00(213)556197617
E-mail address: aeknad@yahoo.fr

http://dx.doi.org/ 10.5281/zenodo.4279147

nanofluid.

Note that the Brownian motion is not taken into consideration in our study, since the nanoparticles size is assumed to be greater than 40 nm.

2. Problem statement

The problem under investigation is a laminar two dimensional mixed convection flow and heat transfer of a non-Newtonian nanofluid, through a heated cavity with openings. The nanofluid consists of a suspension of Ag nanoparticles within a viscoplastic base fluid. This square cavity is assumed to be extended in the third direction Oz, orthogonal to xOy plane. The ventilation is provided by two openings of the same size (We = Ws = 0.2 H), located at the left part of the upper wall and the lower part of the right wall, respectively (Figure 1).

The cold fluid, which is a non-Newtonian viscoplastic nanofluid described by Bingham's rheological law, enters through the opening placed at the top of the left vertical wall and emerges by the other, placed at the bottom of the vertical wall right. All the walls of the cavity are brought to the same temperature, greater than that of the incoming fluid.

X denotes the longitudinal direction and Y the transverse direction, and H denotes the height of the cavity.

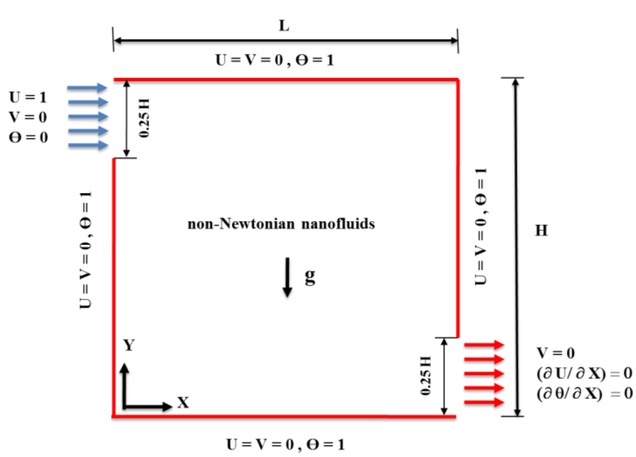

Fig. 1. Physical problem.

The physical properties of the spherical Ag nanoparticles are summarized in Table 1. Constant physical properties are considered for the non-Newtonian nanofluid, whilst the density variation, in the buoyancy term, is determined using the Boussinesq approximation [16].

Table 1. Physical properties of the Ag nanoparticles.

Physical properties	Ag
C_p (J kg^{-1} K^{-1})	230
ρ (kg m^{-3})	10500
k (W m^{-1} K^{-1})	418
β (K^{-1}) 10^5	1.65

3. Mathematical formulation

The nanofluid density ρ_{nf}, the heat capacity $(\rho C_p)_{nf}$, the thermal expansion coefficient $(\rho\beta)_{nf}$, and the thermal diffusivity α_{nf}, may be defined respectively, as follows:

$$\rho_{nf} = (1 - \varphi)\, \rho_f + \varphi\, \rho_s \tag{1}$$

$$(\rho\, C_p)_{nf} = (1 - \varphi)\, (\rho\, C_p)_f + \varphi\, (\rho\, C_p)_s \tag{2}$$

$$(\rho\, \beta)_{nf} = (1 - \varphi)\, (\rho\, \beta)_f + \varphi\, (\rho\, \beta)_s \tag{3}$$

$$\alpha_{nf} = \frac{k_{nf}}{(\rho C_p)_{nf}} \tag{4}$$

For the effective viscosity μ_{nf} and the effective thermal conductivity k_{nf}, the Brinkman [18] and the Maxwell-Garnetts models [19] are employed, respectively:

$$\mu_{nf} = \frac{\mu_f}{(1-\varphi)^{2.5}} \tag{5.a}$$

$$\frac{k_{nf}}{k_f} = \frac{(k_s + 2k_f) - 2\varphi(k_f - k_s)}{(k_s + 2k_f) + \varphi(k_f - k_s)} \tag{5.b}$$

Here, μ_f denotes the apparent viscosity of the base fluid. In our work we consider the case of a Bingham fluid for which, the constitutive model according to Papanastasiou model is written as follows:

$$\mu_f = \mu_0 + \frac{\tau_0}{\dot{\gamma}}\left[1 - \exp(-m\dot{\gamma})\right] \tag{6}$$

Where $\dot{\gamma}$ is the second invariant of the rate-of-strain tensor, m the exponential growth parameter (m = 1000 [20, 21]), τ_0 the Bingham yield stress and μ_0 is the plastic viscosity.

The dimensionless equations, describing the transport phenomenon inside the square cavity, can be written as follows:

$$\nabla \vec{V}' . = 0 \tag{7}$$

$$\frac{\partial \vec{V}'}{\partial t} + \left(\vec{V}' . \vec{\nabla}\right)\vec{V}' = -\vec{\nabla}P + \frac{\mu_{nf}}{Re\rho_{nf}\,\alpha_f}\nabla^2\vec{V}' + \frac{(\rho\beta)_{nf}}{\rho_{nf}\,\beta_f}Ri\,\theta \tag{8}$$

$$\frac{\partial \theta}{\partial t} + \left(\vec{V}' . \vec{\nabla}\right)\theta = \frac{1}{RePr}\frac{\alpha_{nf}}{\alpha_f}\nabla^2\theta \tag{9}$$

Where V' is the velocity dimensionless component. Ri ($= Gr / Re^2$) is the Richardson number, Pr ($= \nu_f / \alpha_f$) is the Prandtl number.

4. Numerical Approach

The Lattice Boltzmann approach uses the particle distribution functions f(x, t), which signifies the probability of the presence of a large number of particles at site x and time t in the mesoscopic system. Consequently, the geometry is covered by lattices, which include a system of particles with symmetrical properties, to satisfy the macroscopic domain with the rotation invariance. Generally, LBM includes two phases; the first phase is streaming in that a group of particles transfer on the lattice link according to the directional velocities by which the velocity space is described. The other step is collision, where particles on the same lattice redistribute and relax into their quasi-equilibrium. The overall lattice Boltzmann equation is defined as follows [20, 21]:

$$\frac{\partial \vec{f}}{\partial t} + \vec{c}\,\nabla\vec{f} = \left(\frac{\partial \vec{f}}{\partial t}\right)_{scat} \tag{10}$$

where f(x,c,t) is the distribution function depending on the particle velocity C at a location (x) and a time (t).

For the flow field, the MRT-LB equation with an explicit treatment of the forcing term C_i can be written in general as the following [22]:

$$f_i(x + e_i\delta_t, t + \delta_t) - f_i(x,t) = -M^{-1}S\left[m_i(x,t) - m_i^{(eq)}(x,t)\right] + C_i \tag{11}$$

Where S is the collision operator given by $S = \mathrm{diag}(s_0, s_1, s_2, s_3, s_4, s_5, s_6, s_7, s_8)$, m = Mf the moment vector, $m^{(eq)}$ = $Mf^{(eq)}$ the equilibria in moment space and M is a orthogonal transformation matrix. For the D_2Q_9 model with standard two dimensional, nine velocities square lattice for flow part is used in this work. The nine discrete velocities {ei, i= 0, 1, ..., 8} are given by [32]:

$$\begin{aligned} &e_0 = (0,0) \\ &e_1 = (1,0)\,;\, e_2 = (0,1)\,;\, e_3 = (-1,0)\,;\, e_4 = (0,-1) \\ &e_5 = (1,1)\,;\, e_6 = (-1,1)\,;\, e_7 = (-1,1)\,;\, e_8 = (1,-1) \end{aligned} \tag{12}$$

For the temperature fields, the MRT-LB equation, based on the D_2Q_5 model, is introduced to solve the advection–diffusion, and its equations can be defined as:

$$g_i(x + e_i\delta_t, t + \delta_t) - g_i(x,t) = -N^{-1}\Theta\left[n_i(x,t) - n_i^{(eq)}(x,t)\right] \tag{13}$$

Where N is a 5 × 5 orthogonal transformation matrix and Θ is a diagonal relaxation matrix. The boldface symbols, g, n and n(eq) are 5-dimensional column vectors g, gi(x, t) = (g0(x, t), g1(xk, t), ..., g4(x, t)), where gi(x, t) is the temperature distribution function.

The five discrete velocities {e_i|i = 0, 1, ..., 4} of the D_2Q_5 model are given by:

$$e_0 = (0,0), e_1 = (1,0)\,;\, e_2 = (0,1)\,;\, e_3 = (-1,0)\,;\, e_4 = (0,-1)$$

5. Results and Discussion

The presented results are generated for various dimensionless groups; such as: the Richardson number ($0.01 \le Ri \le 100$), the Bingham number ($0 \le Bn \le 20$), the Prandtl number ($1 \le Pr \le 30$) and for various solid volume fraction (0% to 10%).

The predicted hydrodynamic and thermal fields' variables are presented, using the Streamlines and temperature Iso-surfaces. The mean transfer rate is also presented, in order to supply useful information about the influence of each parameter, quoted above, on heat transfer exchange within the cavity.

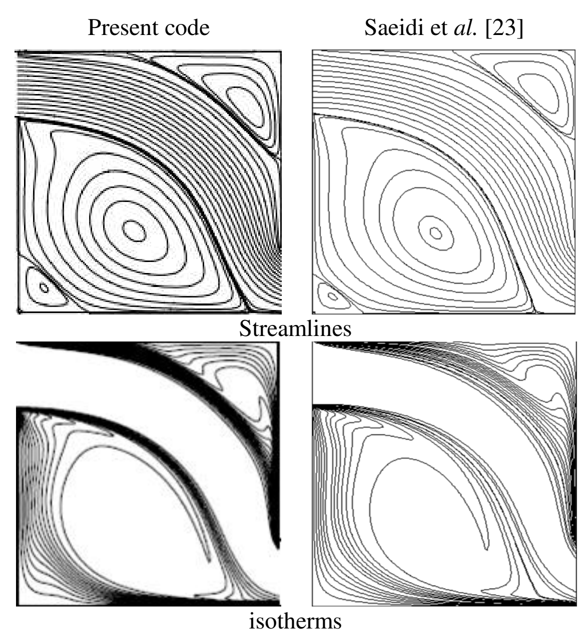

Fig. 2. Comparison of streamlines and isotherms obtained by Saeidi et Khodadadi [23] with those of the present code. Re = 500.

In order to verify the reliability of our computer code, we compared our results with other numerical ones, namely those of Saeidi and Khodadadi [23] as well as Souritiji et *al.* [27] which considered the case of the flow of a Newtonian nanofluid in a ventilated square cavity.

This comparison is illustrated through Figures 2 and 3, which represent streamlines and isotherms as well as the Nusselt number along the hot walls, respectively. These figures show a good agreement between both results.

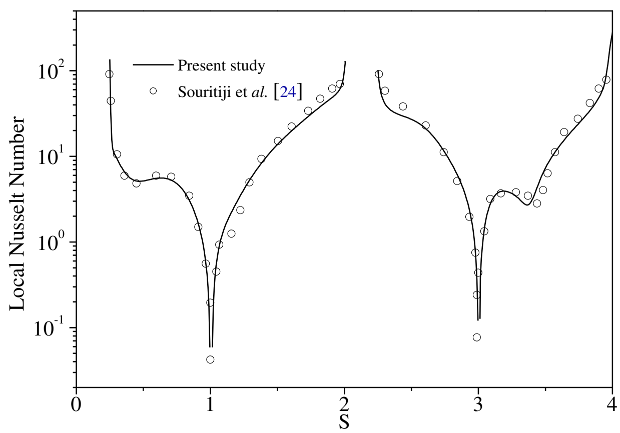

Fig. 3. Local Nusselt number on the four walls of the cavity.

Regarding the mean Nusselt number, a comparison between our results and those of [23] is shown in Table 2. As it ca be seen, the difference between both results does not exceed 4% at most.

Table 2. Average Nusselt number obtained with our computer code and those of reference [23].

Re	S_0	Saeidi and Khodadadi [23]	Present Work	deviation (%)
100	2.125	9.865	9.777	0.900
	0.875	8.558	8.259	3.620
40	2.075	7.924	8.222	3.625
	0.925	7.425	7.363	0.842

Convection mode impact

As far as the Richardson number is concerned, Figure 4 displays the streamlines (a) and the isotherms (b), for various convection modes. We note that for Ri = 0.01 (corresponding to the case of a dominant forced convection), the flow of the fluid in the cavity is generated by the central main flow due to the intensity of inertia force. A large clockwise rotating cell occupies the lower part of the cavity and another cell, smaller than the first one, at its upper right corner.

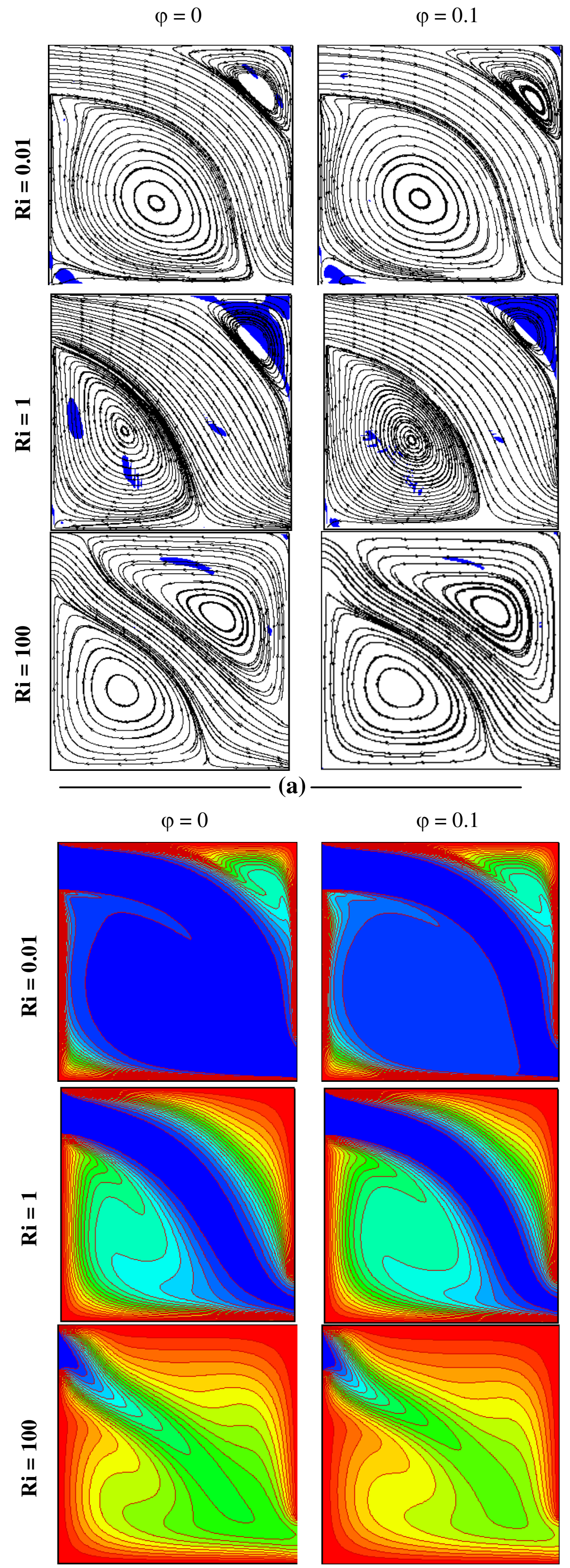

(b)

Fig. 4. Streamlines (a) and isotherms (b) for various values of the Richardson number. Bn = 2, Pr =10.

By increasing the Richardson number, we notice the decrease of the size of the large cell and the increase of the size of the upper one. This is due to a slight weakening of the central flow because of the equality between the inertia and buoyancy forces for Ri = 1 on one hand and the low inertia force compared to the buoyancy force for Ri = 100 on the other hand.

In terms of heat transfer, the structure of the isotherms show that the wall heat exchanges are more intense for forced and mixed convection modes, for which the inertia forces improves, proportionally the thermal wall gradients.

On the other hand, in the case of a dominant natural convection, the wall heat exchanges are very weak, due to the small differences between the wall temperature and that of the fluid wall layers. Note, however, that the heat invades a large part of the cavity, given the convection currents.

Prandtl number impact

Figure 5 illustrates the streamlines and isotherms for different values of the Prandtl number, for the case of a mixed convection mode.

Whatever the value of the Prandtl number, the streamlines show that the incident flow generates the appearance of two recirculation zones, which remain the same size, by increasing the Prandtl number. Indeed, in mixed convection mode (Ri = 1), the hydrodynamic structure is not affected by the Prandtl number variations.

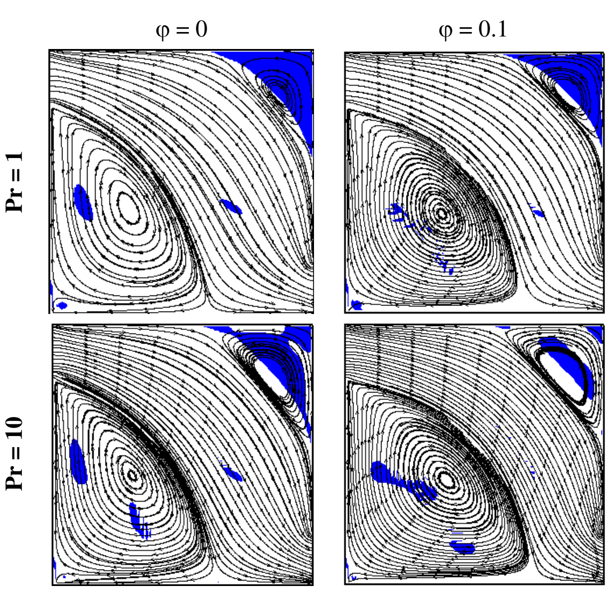

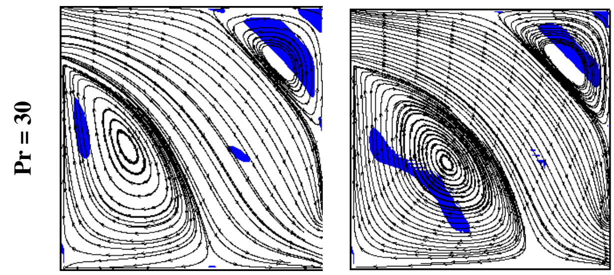

(a)

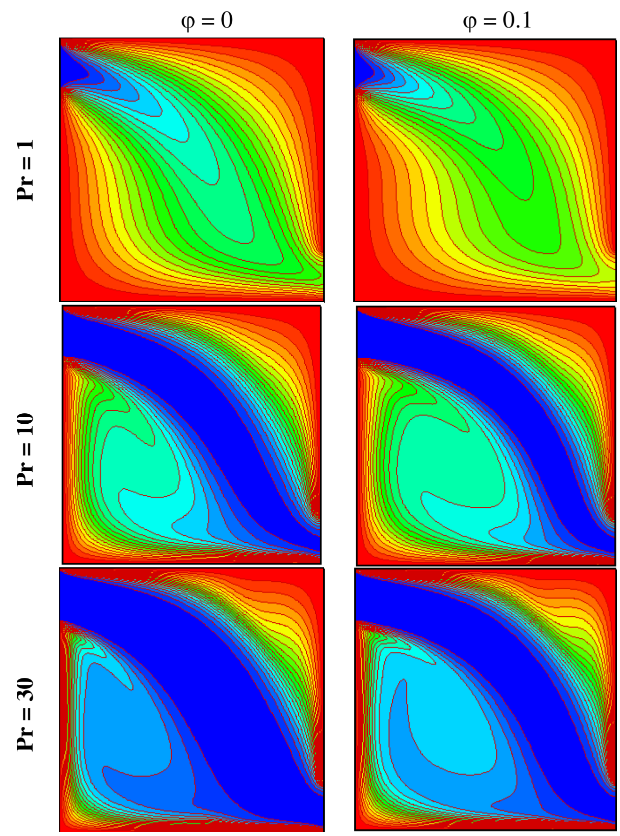

(b)

Fig. 5. Streamlines (a) and isotherms (b) for various values of the Prandtl number. Bn = 2, Ri = 1.

On the other hand, for low values of the Prandtl number (Pr = 1), the isotherms show a rapid warming of the cold fluid because of the low viscosity of the latter, which facilitates the transfer phenomenon.

We find that increasing the Prandtl number improves heat transfer. There is a strong temperature gradient at the interface of the cold fluid and a narrowing of the isotherms at this level, as the Prandtl number increases.

Bingham number effect

In this section, we highlight the effect of the Bingham number on hydrodynamic and thermal structures of the nanofluide flow. Figure 6 displays, for Pr = 10 and Ri = 1, the streamlines, isotherms and unyielded zones for several values of the Bingham number, by considering two nanoparticle volume fractions: φ = 0 and φ = 0.10.

As seen previously, the streamlines show that the main flow generates two recirculation zones: in the lower left part of the cavity (the most important, turning clockwise) and in the upper right part (the less important, turning counterclockwise).

Finally, the increase in the Bingham number decreases the size of the two recirculation zones and increases the extent of the unyielded zones, given the rise in the apparent viscosity which consequently, limits the mobility of the fluid masses.

On the other hand, the isotherms are less curved, as the Bingham number increses and then become almost parallel, denoting a heat transfer by conduction mode.

φ = 0 φ = 0.1

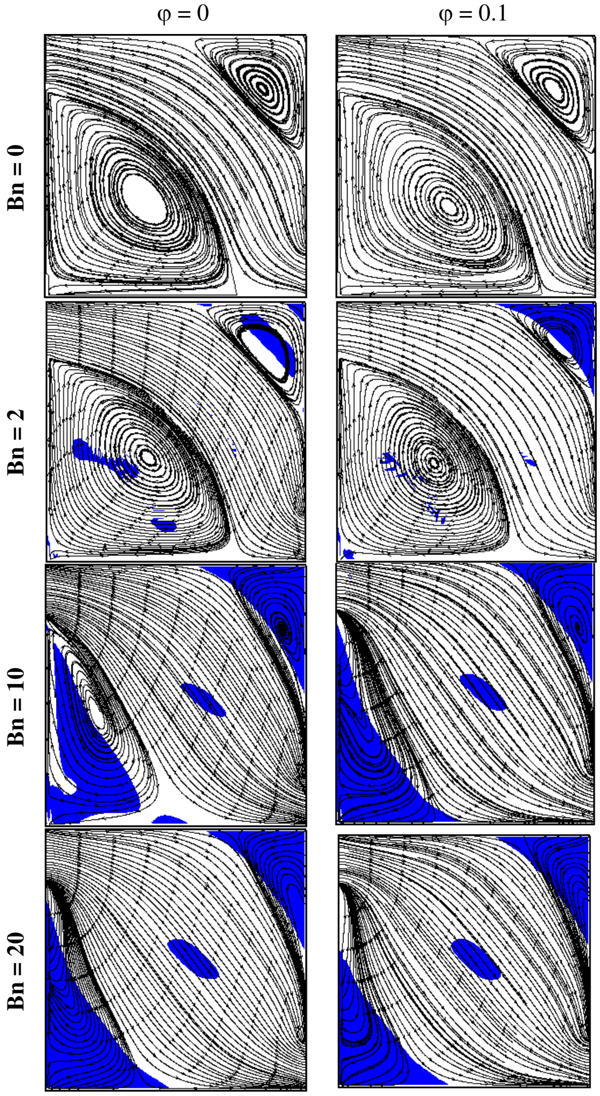

(a)

φ = 0 φ = 0.1

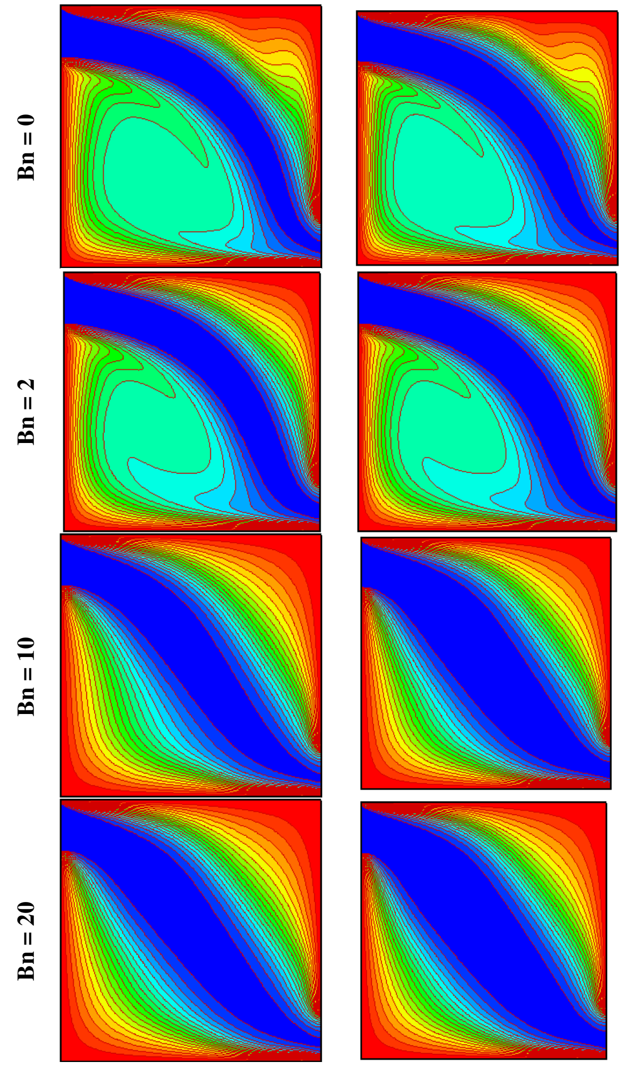

(b)

Fig. 6. Streamlines (a) and isotherms (b) for various values of the Bingham number. Pr = 10, Ri = 1.

Nanoparticles volume fraction impact

Figure 7 shows the evolution of the Nusselt number, averaged along the four walls of the cavity, as a function of the nanoparticles volume fraction φ (φ = 0 to 0.1) and for the three convection modes (Ri = 0.01, 1 and 100).

As it can be seen, whatever the convection mode, the average Nusselt number increases lineary as a function of φ, such that the best transfer rates are displayed by the dominant forced convection mode (Ri = 0.01), which differ significantly from those corresponding to the mixed convection mode (Ri = 1), then those of the dominant natural convection (Ri = 100).

Finally, it is interesting to note that for a nanoparticles volume fraction equal to 10%, the transition from a dominant forced convection mode to a mixed one decreases the heat transfer rate by 73.02% and 89.16%, by switching to the dominant natural convection mode.

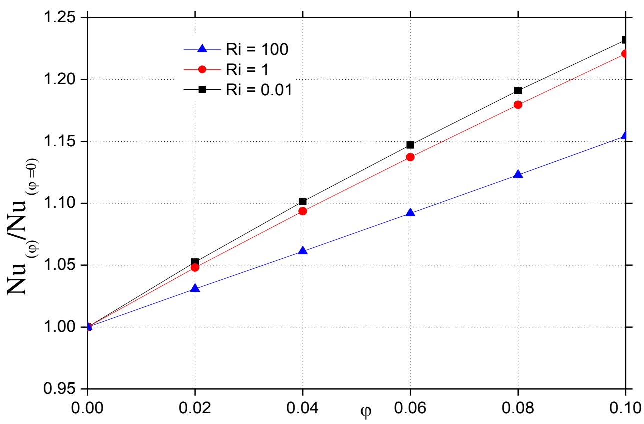

Fig. 7. Variation of the mean Nusselt number as a function of the nanoparticles volume fraction for the three convection modes. Bn = 2, Pr =10.

6. Conclusion

In this work, a square ventilated cavity subjected to mixed laminar convection has been investigated numerically using the LBM application and by taking into account the impact of various pertinent parameters: the Richardson number, the Bingham number and the Prandtl number, side by side with the nanoparticles volume fraction. The results show that heat transfer is very significant when dispersing solid nanoparticles into the base fluid and is improved by increasing their volume fraction. The results show also that the increase in of the both Richardson and Bingham numbers decreases the heat transfer rate, unlike the Prandtl number whose increase promotes heat exchanges within the cavity.

NOMENCLATURE

a	Coefficient in external forces (= g β)
c	Cold
c_s	Sound velocity in the Lattice ($= 1/\sqrt{3}$)
C_p	Specific heat at constant pressure, (J kg^{-1} K^{-1})
f	fluid
f_{eq}	Equilibrium distribution Function
F_{ext}	External Force
fi	Distribution Function
h	Hot
k	Thermal conductivity, (W m^{-1} K^{-1})
H,x,y	Enclosure dimensions, (m)
m_j	Moments
n_f	Nanofluid
Nu	Mean Nusselt number
Pr	Prandtl number (Pr = ν/α)
s	Solid particles
S_j	Relaxation rate
t	Time, (s).
T	Temperature, (K)
Ri	Richardson number,
u	Horizontal velocity component, (m)
v	Vertical velocity component, (m)
x, y	Dimensional Cartesian coordinates, (m)
Greek letters	
α	Thermal diffusivity, (m^2 s^{-1})
β	Thermal expansion coefficient, (K^{-1})
θ	Dimensionless temperature
ωi	Coefficients of the equilibrium function
ρ	Density, (kg m^{-3})
φ	Nanoparticles volume fraction
ε	Energy square
ν	Kinematic viscosity, (m^2 s^{-1})
Ω	Collision Operator

Conflict of Interest

The authors declare no conflict of interest, financial or otherwise.

References

[1] Boutra, A. Ragui, K. and Benkahla, Y.K (2015) Numerical study of mixed convection heat transfer in a lid-driven cavity filled with a nanofluid. Mechanics & Industry, 16 (5): 505.

[2] Boutra, A. Ragui, K. Labsi, N. and Benkahla, Y.K, (2015) Lid-driven and inclined square cavity filled with a nanofluid: Optimum heat transfer, Open Eng. 5:248-255.

[3] Nasreddine O., Cheikh N.B. (2009) Mixed convection in a double lid-driven cubic cavity, Int. J. Thermal Sciences, 48: 1265-1272.

[4] Guo, G., and Sharif, M. A. R., (2004), Mixed Convection in Rectangular Cavities at Various Aspect Ratios with Moving Isothermal Sidewalls and Constant Flux Heat Source on the Bottom Wall, International Journal of Thermal Science, Vol. 43, pp. 465-475.

[5] Cheng, T. S. (2011) Characteristics of Mixed Convection Heat Transfer in a Lid-Driven Square Cavity with various Richardson and Prandtl Numbers, International Journal of Thermal Sciences, Vol. 50, pp. 197-205.

[6] Zhao, M., Yang, M., Lu, M., and Zhang, Y. (2011) Evolution to Chaotic Mixed Convection in a Multiple Ventilated Cavity, International Journal of Thermal Sciences, Vol. 50, pp. 2464-2472.

[7] Mahmoudi, A. H., Shahi, M., and Talebi, F.(2010) Effect of inlet and outlet Location on the Mixed Convective Cooling Inside the Ventilated Cavity Subjected to an External Nanofluid, International Communications in Heat and Mass Transfer, Vol. 37, pp. 1158-1173.

[8] Sourtiji, E., Hosseinizadeh, S. F., Gorji-Bandpy, M., and Ganji, D. D.(2011) Effect of Water-Based Al2O3 Nanofluids on Heat Transfer and Pressure Drop in Periodic Mixed Convection Inside a Square Ventilated Cavity, International Communications in Heat and Mass Transfer, Vol. 38, pp. 1125-1134.

[9] Sourtiji, E., Hosseinizadeh, S. F., Gorji-Bandpy, M., and Khodadadi, J. M. (2011) Computational Study of Turbulent Forced Convection Flow in a Square Cavity with Ventilation Ports, Numerical Heat Transfer, Part A, Vol. 59, Issue 12, pp. 954-969.

[10] R. Kamali, A.R. Binesh, (2010) Numerical investigation of heat transfer enhancement using carbon nanotube-based non-Newtonian nanofluids, Int. Commun. Heat Mass Transfer 37, 1153–1157.

[11] M. Moawed, W. El-Maghlany, R.K. Ali, M. Hamed, (2014) Forced convection heat transfer inside tube for non-Newtonian fluid flow utilizing nanofluid, Int. J. Appl. Sci. Eng.Res. 3, 889–898.

[12] M. Hojjat, S.G. Etemad, R. Bagheri, J. Thibault, (2011) Convective heat transfer of non-Newtonian nanofluids through a uniformly heated circular tube, Int. J. Therm. Sci. 50, 525–531.

[13] S. Ouyahia, Y.K, Benkahla,W. Berabou, A. Boudiaf, (2017) Numerical study of the flow in a square cavity filled with Carbopol-TiO2 nanofluid, Powder Technology. 311, 101–111.

[14] Boutra A, Ragui K, Labsi N, Bennacer R, Benkahla YK (2016) Natural Convection Heat Transfer of a Nanofluid into a Cubical Enclosure: Lattice Boltzmann Investigation. Arabian Journal for Science and Engineering, 41: 1969-1980.

[15] Boutra A, Ragui K, Bennacer R, Benkahla YK (2016) Three-dimensional fluid flow simulation into a rectangular channel with partitions using the lattice-Boltzmann method. eur. phys. j. appl. phys 74: 24612.

[16] Boutra A, Ragui K, Bennacer R, Benkahla YK (2017) Free Convection Heat Transfer of Nanofluids into Cubical Enclosures with a Bottom Heat Source: Lattice Boltzmann Application. Energy Procedia, 139: 217-223.

[17] Bejan, A (2004) Convection heat transfer, John Wiley & Sons, Inc., Hoboken, New jersey, USA.

[18] Brinkman, H.C (1952), The viscosity of concentrated suspensions and solutions, J. Chem. Physics, 20: 571-581.

[19] Maxwell J.C. (1873) A Treatise on Electricity and Magnetism, Vol. II, Oxford University Press, Cambridge, U K, 54.

[20] A. Boutra, Y.K. Benkahla, DE. Ameziani, R. Bennacer. (2017) Lattice Boltzmann simulation of natural convection in cubical enclosures for Bingham plastic fluid ». Heat Transfer Research 48(7), pp 607-624.

[21] Mitsoulis, E. and Zisis, T., (2001) Flow of Bingham plastics in a lid-driven square cavity, J. Non-Newtonian Fluid Mech, 101, pp. 173-180.

[22] Bouarnouna, K., Boutra, A., Ragui, K., Labsi, N., Benkahla, Y.K. (2019) Multiple-Relaxation-Time Lattice Boltzmann Model for Flow and Convective Heat Transfer in Channel with Porous Media». Journal of Statistical Physics, 126 , 1–20.

[23] Saeidi, S. M. Khodadadi, J. M. (2006) Forced convection in a square cavity with inlet and outlet ports, International Journal of Heat and Mass Transfer 49 1896–1906.

[24] Souritiji, E. Gorji-Bandpy, M. Ganji, D.D. Hosseinizadeh, S.F. (2014) Numerical analysis of mixed convection heat transfer of Al2O3-water nanofluid in a ventilated cavity considering different positions of the outlet port, Powder Technology, 262, 71–81.

Recommended Citation

Boutra, A. Benkahla, Y.K. and Labsi, N. (2020) Numerical predictions using LBM application: laminar mixed convection of non-Newtonian nanofluids in ventilated square cavities. Algerian Journal of Chemical Engineering, 01, 31-38.

http://dx.doi.org/10.5281/zenodo.4279147